Electronic Supplementary Material (ESI) for Inorganic Chemistry Frontiers.

Supporting information for

Cooperative Effect of Copper-Induction and AIE Leading to Bright Luminescence of Gold Nanoclusters

Yongjie Zhang,[a, ‡,*] Luyao Feng,[b, ‡] Jingyan Luan,[b] Guomei Zhang,[a] Ning Sheng,[a] Jinglin Shen[b,*]

[a] *School of Chemistry, Chemical Engineering and Materials, Jining University, Qufu, Shandong, 273155, P. R. China*

[b] *School of Chemistry and Chemical Engineering, Qufu Normal University, Qufu, Shandong, 273165, P. R. China*

* *Corresponding authors.*

E-mail addresses: yj_zhang_chemeng@tju.edu.cn (Y. Zhang), jinglinshen@163.com (J. Shen)

‡ *These authors contributed equally to this work.*

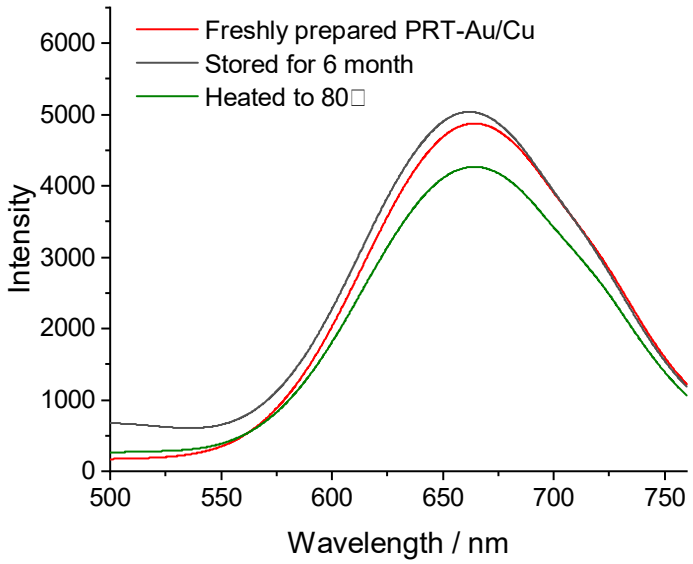

Figure S1. Photoluminescence spectra of **PRT-Au/Cu** composite to show its stability.

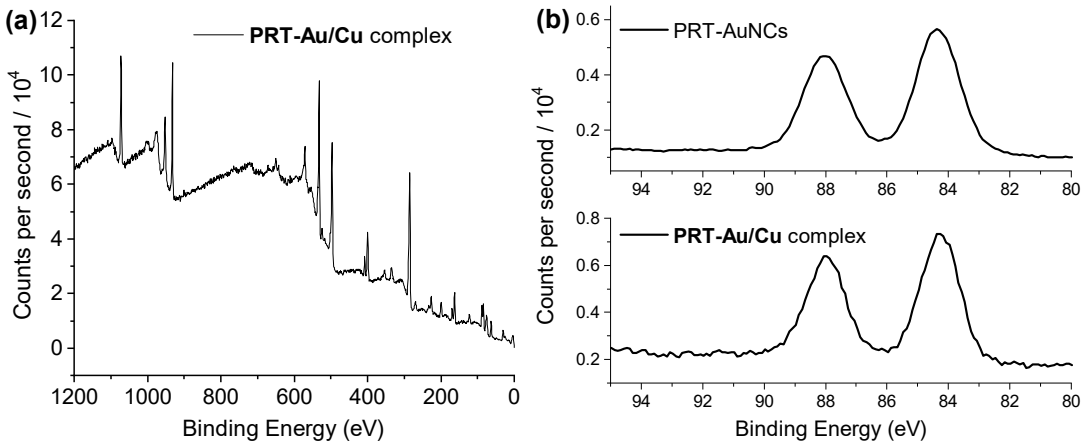

Figure S2. (a) Full spectrum of X-ray photoelectron spectroscopy (XPS) for **PRT-Au/Cu** complex $c[Cu^{2+}]$ = 12 mM; (b) Comparison of Au 4f spectra between PRT-AuNCs and **PRT-Au/Cu** complex.

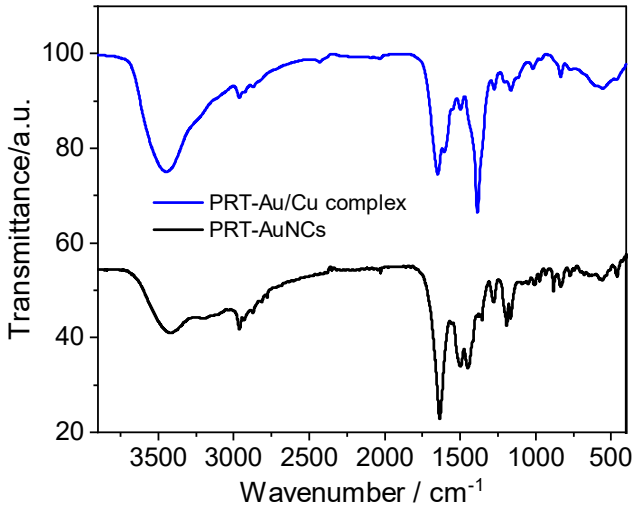

Figure S3. Comparison of FTIR spectra between **PRT-Au/Cu** complex *c*[Cu^{2+}] = 12 mM and primitive PRT-AuNCs

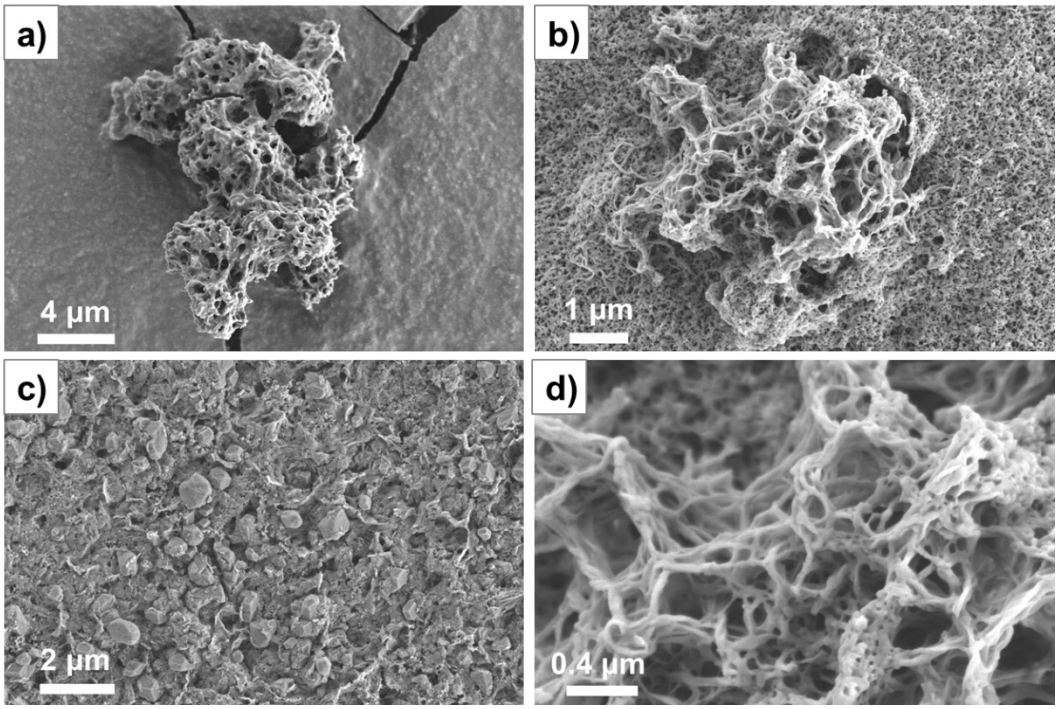

Figure S4. SEM images of PRT-AuNCs/Cu^{2+} systems with addition of (a) 10 mM; (b, d) 14 mM and (c) 16 mM Cu^{2+}.

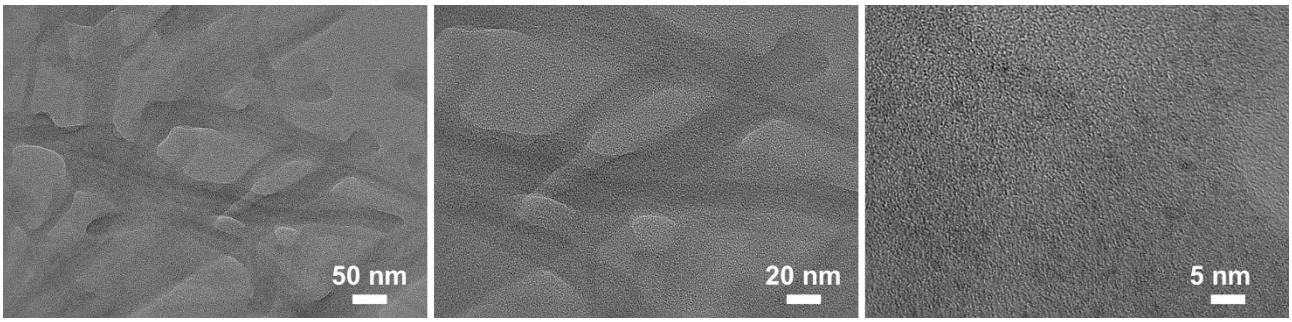

Figure S5. HR-TEM images of **PRT-Au/Cu** composite (c[Cu^{2+}] = 12 mM) at high magnification to show its detailed structure and components.

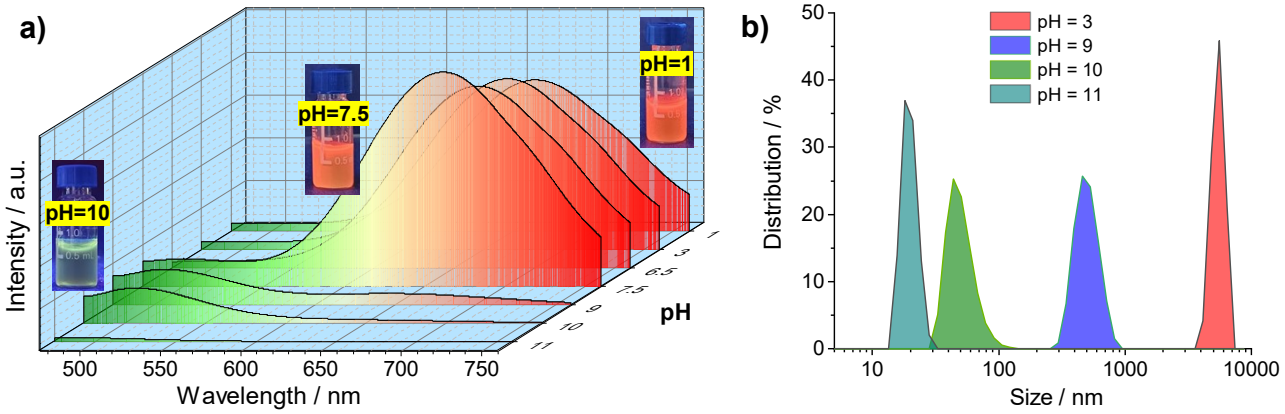

Figure S6. (a) pH-dependent photoluminescence spectra of **PRT-Au/Cu** composite (insets are the photos of samples at different pH under 365 nm UV lamp irradiation); (b) Size distribution of **PRT-Au/Cu** aggregates at different pH measured by dynamic light scattering.

Table S1. Photophysical parameters of PRT-AuNCs and **PRT-Au/Cu** composite in powder state

Species	[a] λ_{Em} / nm	[b] τ_1 / μs	[b] τ_2 / μs	[c] τ / μs
PRT-AuNCs (powder)	615	9.30 (0.9273)	172.04 (0.0727)	21.13
PRT-Au/Cu (powder)	666	11.72 (0.8389)	169.05 (0.1611)	37.07

[a] Maximum emission wavelength.

[b] Components of bi-exponential luminescence lifetimes and pre-exponential factors.

[c] Averaged luminescence lifetimes measured at excitation wavelength of λ_{Ex} = 365 nm.

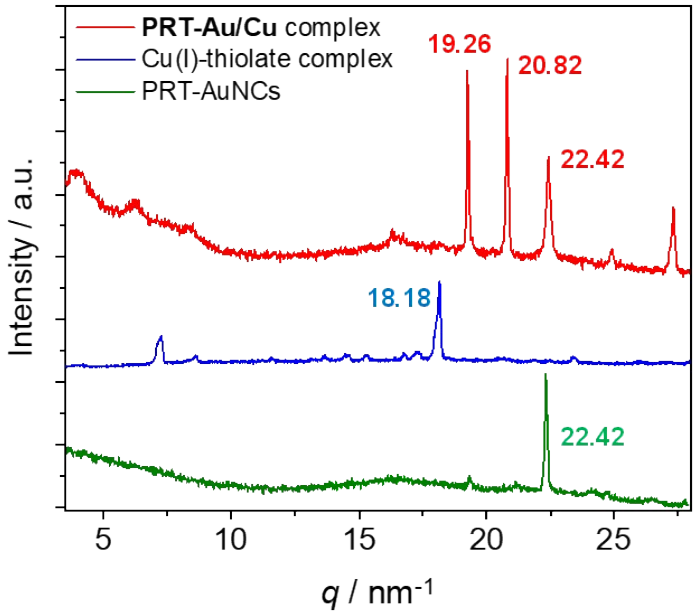

Figure S7. Small angle X-ray scattering patterns of PRT-AuNCs, Cu(I)-thiolate complex and PRT-Au/Cu composite.

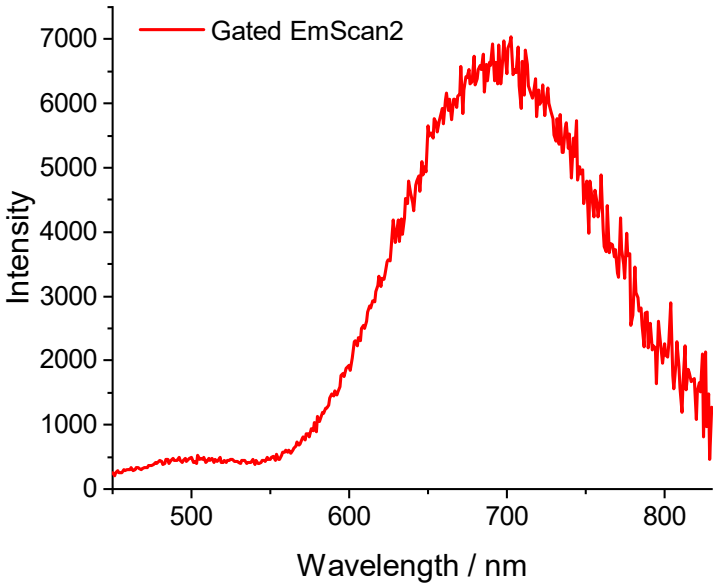

Figure S8. Phospherescent spectra of **PRT-Au/Cu** composite (λ_{Ex} = 385 nm, delay time: 5 μs, gate width: 20 μs).

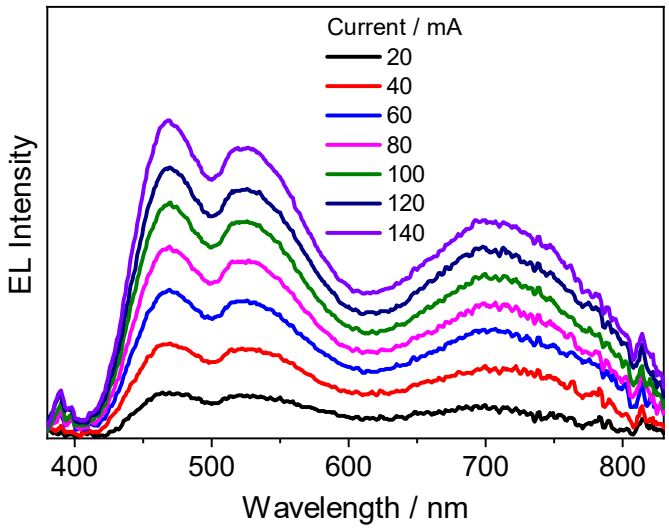

Figure S9. Electroluminescence spectra of the WLED prepared with **PRT-Au/Cu** composite and commercially available $BaMgAl_{10}O_{17}:Eu^{2+}$ and $(Ba,Sr)_2SiO_4:Eu^{2+}$.

Table S2. CIE coordinates and correlated color temperature (CCT) of the prepared WLED at different drive current.

I / mA	CIE *x*	CIE *y*	CCT / K
20	0.2955	0.369	7001
40	0.2949	0.3684	7045
60	0.294	0.3613	7153
80	0.2925	0.3597	7245
100	0.2925	0.3589	7257
120	0.288	0.3613	7448
140	0.2884	0.3604	7433